Smart Mater. Struct. **15** (2006) 1143–1149 doi:10.1088/0964-1726/15/4/028

Effect of small size-scale on the radial buckling pressure of a simply supported multi-walled carbon nanotube

G Q Xie[1,2], X Han[1,4], G R Liu[3] and S Y Long[2]

[1] The Key Laboratory of Advanced Technology for Vehicle Body Design and Manufacture of Ministry of Education, Hunan University, Changsha 410082, People's Republic of China
[2] Department of Engineering Mechanics, Hunan University, Changsha 410082, People's Republic of China
[3] Center for Advanced Computations in Engineering Science, Department of Mechanical Engineering, National University of Singapore, 10 Kent Ridge Crescent, Singapore 119260, Singapore

E-mail: hanxu@hnu.cn

Received 9 August 2005, in final form 24 May 2006
Published 7 July 2006
Online at stacks.iop.org/SMS/15/1143

Abstract
A buckling multiple-shell model of carbon nanotubes subjected to a uniform external radial pressure is suggested based on the theory of nonlocal elasticity. The average (nonlocal) stress incorporating the small size-scale is introduced into the governing equations of the multi-walled carbon nanotubes. A factor for the effect of the small size-scale is obtained, and the relationship of the effect of the small size-scale for a simply supported double-walled carbon nanotube to its size and buckling mode has been investigated. Numerical examples demonstrate the effect of small size-scale.

(Some figures in this article are in colour only in the electronic version)

1. Introduction

Carbon nanotubes (CNTs) are multi-layer cylindrical shells of rolled graphene layers composed of carbon atoms in a periodic hexagonal arrangement. CNTs have shown remarkably high stiffness and radial strength in engineering applications. The references listed herein (Schadler *et al* 1998, Maruyama and Alam 2002, Peigney *et al* 2000) are some examples. Due to their large aspect ratios and small diameters, CNTs have emerged as potentially attractive materials as reinforcing elements in lightweight and high-strength structural composites (Li and Chou 2003b). It is difficult to obtain characterization of nanotubes by experiment. Therefore, the investigation of mechanical behavior of carbon nanotubes mainly focuses on theoretical simulation by using atomistic and continuum models (e.g. Wang and Varadan 2005, Li and Chou 2004) recently dedicated to these research areas. Due to the cost of computation for large-sized atomic systems, practical applications of atomistic modelling techniques are very limited. As a result, it is necessary to develop continuum models which may overcome the limitations of atomistic simulations concerning both time-and size-scales, and which also give reasonable results for small size-scales. So far, a lot of continuum mechanics models have been used to investigate the properties of carbon nanotubes (there are some examples in Wong *et al* 1997 and Li and Chou 2003a).

Buckling of CNTs is an important issue, and works (e.g. Ru 2001, Lourie *et al* 1998) have demonstrated that the classic continuum models can be used to simulate mechanical properties of carbon nanotubes. Peddieson *et al* (2003) pointed out that nanoscale devices would exhibit nonlocal effects and that nonlocal continuum mechanics could potentially play a useful role in analysis related to nanotechnology applications. The theory of nonlocal continuum mechanics was initially proposed by Eringen (1972) and Eringen and Edelen (1972). It is suggested that the stress state at a given point depends on not only the point strain state but also the strain states of the other points in the body, while the local continuum mechanics assumes that the stress state at a given point is only related to the strain state at that point. Thus, the theory of nonlocal continuum mechanics contains information about

[4] Author to whom any correspondence should be addressed.

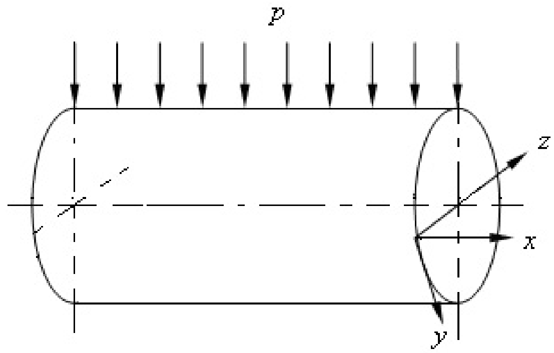

Figure 1. The shell model of a carbon nanotube.

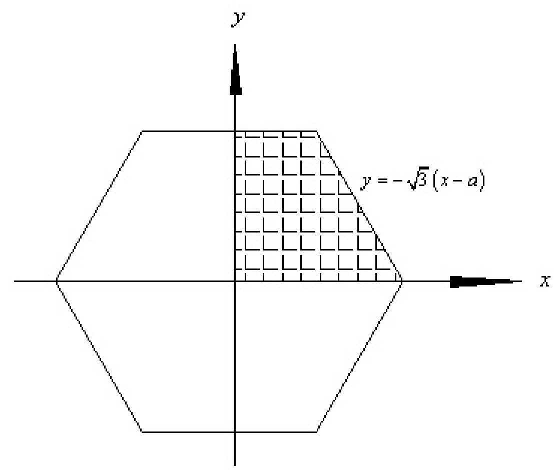

Figure 2. The representative element.

the long-range forces between atoms, and the internal size-scale is introduced into the constitutive equations as a material parameter.

In this paper, the average stress is used in the equilibrium equations, which incorporate information about small size-scale; a nonlocal model of multiple shells is developed for the radial buckling of multi-walled carbon nanotubes.

2. Basic equations of a carbon nanotube

There are a few theories concerning shell; one of the simpler theories for thin shells is that of Love (1888). Some represent a further simplification of the derivation of the thin shell equations as proposed by Love (e.g. Donnell 1933). There is a summary of the thin shell equations of several thin shell theories including: Donnell's theory, Love's theory and an improved theory that includes the effects of rotary inertia and transverse shear in Price *et al* (1998).

Consider the pre-buckling of a multi-walled cylindrical shell (figure 1) subjected to a uniform radial pressure. The radius of the shell is R and the thickness is h. The material of the shell is regarded as homogeneous, isotropic and elastic. The coordinate system is built with its origin in the middle surface of the shell, with the x direction parallel to the axis of the cylinder and the y direction tangent to a circular arc, and the z direction normal to the median surface.

The basic equations of a carbon nanotube are given in terms of nonlocal elastic theory. Due to the long-range force, the stress in a point is dependent on the strains of all the points in the body. The average stress of a representative volume elementary (RVE) (figure 2) is used in the equilibrium equations, which contains the parameter of C–C bond size a. Extracting a right hexagonal prism (the basic unit of a graphene layer) as the RVE, the average stress of RVE can be obtained in terms of a Taylor series.

The stress at point (x, y) can be expanded as

$$\begin{aligned}\tau_{ij}(x,y) &= \tau_{ij}(0,0) + \frac{\partial \tau_{ij}(x,y)}{\partial x}\bigg|_{\substack{x=0\\y=0}} x + \frac{\partial \tau_{ij}(x,y)}{\partial y}\bigg|_{\substack{x=0\\y=0}} y \\ &\quad + \frac{1}{2!}\frac{\partial^2 \tau_{ij}(x,y)}{\partial x^2}\bigg|_{\substack{x=0\\y=0}} x^2 + \frac{1}{2!}\frac{\partial^2 \tau_{ij}(x,y)}{\partial y^2}\bigg|_{\substack{x=0\\y=0}} y^2 \\ &\quad + \frac{1}{2!}\frac{\partial^2 \tau_{ij}(x,y)}{\partial xy}\bigg|_{\substack{x=0\\y=0}} xy + \cdots \end{aligned} \tag{1}$$

where $\tau_{ij}(x, y)$ is the nonlocal stress tensor, and $\tau_{ij}(0, 0)$ is the local stress tensor.

To take the average of $\tau_{ij}(x, y)$ in RVE, in terms of the symmetry of the representative volume element, we have

$$\begin{aligned}\langle \tau_{ij}(x,y)\rangle &= \left\{\int_{\mathrm{RVE}}\left[\tau_{ij}(0,0) + \frac{\partial \tau_{ij}(x,y)}{\partial x}\bigg|_{x=0,y=0} x \right.\right. \\ &\quad + \frac{\partial \tau_{ij}(x,y)}{\partial y}\bigg|_{x=0,y=0} x + \frac{\partial^2 \tau_{ij}(x,y)}{2\partial x^2}\bigg|_{x=0,y=0} x^2 \\ &\quad \left.\left. + \frac{\partial^2 \tau_{ij}(x,y)}{2\partial y^2}\bigg|_{x=0,y=0} y^2\right] h\,\mathrm{d}x\,\mathrm{d}y\right\}\left\{\int_{\mathrm{RVE}} h\,\mathrm{d}x\,\mathrm{d}y\right\}^{-1} \\ &= \tau_{ij}(0,0) + \left\{\frac{\partial^2 \tau_{ij}(x,y)}{2\partial x^2}\bigg|_{x=0,y=0} 4h \right. \\ &\quad \times \int_0^{\frac{\sqrt{3}}{2}a}\mathrm{d}y \int_0^{-\frac{\sqrt{3}}{3}y+a} x^2\,\mathrm{d}x \\ &\quad \left. + \frac{\partial^2 \tau_{ij}(x,y)}{2\partial y^2}\bigg|_{x=0,y=0} 4h \int_0^{\frac{\sqrt{3}}{2}a} y^2\,\mathrm{d}y \int_0^{-\frac{\sqrt{3}}{3}y+a}\mathrm{d}x\right\} \\ &\quad \times \left\{4h\int_0^{\frac{\sqrt{3}}{2}a}\mathrm{d}y\int_0^{-\frac{\sqrt{3}}{3}y+a}\mathrm{d}x\right\}^{-1} \\ &= \tau_{ij}(0,0) + 0.208a^2\frac{\partial^2 \tau_{ij}(x,y)}{\partial x^2}\bigg|_{x=0,y=0} \\ &\quad + 0.208a^2\frac{\partial^2 \tau_{ij}(x,y)}{\partial y^2}\bigg|_{x=0,y=0} \\ &= (1+0.208a^2\nabla^2)\tau_{ij}(0,0). \end{aligned} \tag{2}$$

Equation (2) can be expressed approximately as

$$\boldsymbol{\sigma} = \langle \boldsymbol{\tau}\rangle = (1+0.208a^2\nabla^2)\boldsymbol{\tau}. \tag{3}$$

Inversion of equation (3) yields

$$\boldsymbol{\tau} = (1-0.208a^2\nabla^2)\boldsymbol{\sigma}. \tag{4}$$

The stress–strain relation of the carbon nanotube's shell, considering the effects of small size-scale, is given by

$$(1-0.208a^2\nabla^2)\boldsymbol{\sigma} = \mathbf{C} : \boldsymbol{\varepsilon} \tag{5}$$

where **C** is the elastic stiffness matrix of classical isotropic elasticity. If the small size a vanishes, equation (5) reverts to Hooke's law.

The stress function φ is given as

$$\sigma_1 = \frac{1}{R^2}\frac{\partial^2\varphi}{\partial\theta^2}, \qquad \sigma_2 = \frac{\partial^2\varphi}{\partial x^2}, \qquad \sigma_{12} = -\frac{1}{R}\frac{\partial^2\varphi}{\partial x\partial\theta}. \tag{6}$$

Substituting equation (5) into the geometric equations, the physical equations and the equilibrium equations of a carbon nanotube shell, and combining these equations into equation (6), we can obtain

$$\begin{aligned}\frac{D}{h}\nabla_R^4 u_3 &= \frac{1}{R^2}\frac{\partial^2\varphi}{\partial\theta^2}\frac{\partial^2 u_3}{\partial x^2} + \frac{1}{R^2}\frac{\partial^2\varphi}{\partial x^2}\frac{\partial^2 u_3}{\partial\theta^2} - 2\frac{1}{R^2}\frac{\partial^2\varphi}{\partial x\partial\theta}\frac{\partial^2 u_3}{\partial x\partial\theta}\\ &+ \frac{1}{R}\frac{\partial^2\varphi}{\partial x^2} - \frac{0.208Da^2}{h}\left[\frac{\partial^6 u_3}{\partial x^6} + \frac{1}{R^6}\frac{\partial^6 u_3}{\partial\theta^6}\right.\\ &\left.+ \frac{(2-\nu)}{R^2}\left(\frac{\partial^6 u_3}{\partial x^4\partial\theta^2} + \frac{1}{R^2}\frac{\partial^6 u_3}{\partial\theta^4\partial x^2}\right)\right] + \frac{T}{h}\end{aligned} \tag{7}$$

where the algorithm ∇_R^2 is given as

$$\nabla_R^2 = \frac{1}{R^2}\frac{\partial^2}{\partial\theta^2} + \frac{\partial^2}{\partial x^2},$$

D is the effective bending stiffness of the shell, u_3 is the deflection in the z direction, and T is the normal inward external force on the shell.

Neglecting the nonlinear terms, the consistent equation for the cylindrical middle surface is (Cheng 1989)

$$\frac{1}{E}\nabla_R^4\varphi = -\frac{1}{R}\frac{\partial^2 u_3}{\partial x^2}. \tag{8}$$

Appling the algorithm ∇_R^4 to equation (7) yields

$$\begin{aligned}&\frac{D}{h}\nabla_R^8 u_3 + \frac{E}{R^2}\frac{\partial^4 u_3}{\partial x^4} + \sigma_1\nabla_R^4\left(\frac{\partial^2 u_3}{\partial x^2}\right)\\ &+ \sigma_2\frac{1}{R^2}\nabla_R^4\left(\frac{\partial^2 u_3}{\partial\theta^2}\right) + 2\sigma_{12}\nabla_R^4\left(\frac{1}{R}\frac{\partial^2 u_3}{\partial x\partial\theta}\right)\\ &+ \frac{1}{h}0.208a^2 D\nabla_R^4\xi - \frac{\nabla_R^4 T}{h} = 0\end{aligned} \tag{9}$$

where equation (8) is adopted,

$$\xi = \frac{\partial^6 u_3}{\partial x^6} + \frac{1}{R^6}\frac{\partial^6 u_3}{\partial\theta^6} + \frac{(2-\nu)}{R^2}\left(\frac{\partial^6 u_3}{\partial x^4\partial\theta^2} + \frac{1}{R^2}\frac{\partial^6 u_3}{\partial\theta^4\partial x^2}\right).$$

During elastic pre-buckling, the magnitudes of the initial middle-surface radial forces are much larger than the bending force. Equation (9) is reduced as

$$\begin{aligned}&D\nabla_R^8 u_3 + \frac{Eh}{R^2}\frac{\partial^4 u_3}{\partial x^4} + \frac{p_2^0}{R}\nabla_R^4\left(\frac{\partial^2 u_3}{\partial\theta^2}\right)\\ &+ 0.208a^2 D\nabla_R^4\xi - \nabla_R^4 T = 0\end{aligned} \tag{10}$$

where p_2^0 is a uniform external radial pressure on a carbon nanotube.

3. Buckling analysis

Multi-walled carbon nanotubes possess a hollow multilayer structure which interacts with the adjacent tubes by van der Waals forces. For linear infinitesimal buckling, the net van der Waals pressure at any point between adjacent tubes should be a linear function of the difference in deflection at that point (Ru 2000). Assume that $T_{i(i+1)}$ denotes the pressure on tube i due to tube $i+1$, which is positive inward and can be described by

$$T_{(i+1)i} = c_i(u_3^{(i)} - u_3^{(i+1)}) \qquad (i = 1, 2, \ldots, N) \tag{11}$$

where the subscripts $1, 2, \ldots, N$ represent the numbers of the tube. w_i is the (inward) deflection of tube i, and the van der Waals interaction coefficient c_i can be estimated by (Yoon *et al* 2003a)

$$c_i = \frac{400R_i}{0.16d^2}\ \text{erg cm}^{-2}, \qquad d = 0.142\ \text{nm}. \tag{12}$$

Letting $T_{(i+1)i}$ stand for the pressure on tube $i+1$ due to tube i, we can obtain

$$T_{(i+1)i} = -\frac{R_i}{R_{i+1}}T_{i(i+1)} \tag{13}$$

where R_i is the radius of tube i.

Applying equation (10) to each concentric tube of a multi-walled carbon nanotube, we can obtain

$$\begin{aligned}D\nabla_j^8 u_3^{(j)} &= \nabla_j^4\left[T_{j(j+1)} - \frac{R_{j-1}}{R_j}T_{(j-1)j} - 0.208a^2\nabla_j^4\xi_j\right.\\ &\left.+ \frac{p_2^{0(j)}}{R_j^2}\frac{\partial^2}{\partial\theta^2}\nabla_j^4 u_3^{(j)} - \frac{Eh}{R_j^2}\frac{\partial^4 u_3^{(j)}}{\partial x^4}\right]\end{aligned} \tag{14}$$

where

$$\xi_j = \frac{\partial^6 u_3^{(j)}}{\partial x^6} + \frac{1}{R_j^6}\frac{\partial^6 u_3^{(j)}}{\partial\theta^6} + \frac{(2-\nu)}{R_j^2}\left(\frac{\partial^6 u_3^{(j)}}{\partial x^4\partial\theta^2} + \frac{1}{R_j^2}\frac{\partial^6 u_3^{(j)}}{\partial\theta^4\partial x^2}\right),$$

$j = 2, 3, \ldots, N$

represents the jth number of the tube. ∇_j^2 is

$$\nabla_j^2 = \frac{\partial^2}{\partial x^2} + \frac{1}{R_j^2}\frac{\partial^2}{\partial\theta^2}.$$

Under uniform external radial pressure P, the membrane forces $p_2^{0(j)}$ prior to buckling are constants. It follows from the equilibrium condition prior to buckling that

$$p_2^{0(j)} = -p_j^0 R_j \tag{15}$$

where p_j^0 denotes the net (inward) normal pressure to the tube j prior to buckling. In addition, the radial equilibrium condition prior to buckling gives

$$p_j^0 = -Eh\frac{\Delta R_j}{R_j^2} \tag{16}$$

where ΔR_j is the radial (inward) displacement of the jth tube. The following expressions can be obtained:

$$p_1^0 = p_{12}^0 = c_1(\Delta R_2 - \Delta R_1) \tag{17a}$$

$$\begin{aligned}p_k^0 &= p_{k(k+1)}^0 - \frac{R_{k-1}}{R_k}p_{(k-1)k}^0 = c_k\left[(\Delta R_{k+1} - \Delta R_k)\right.\\ &\left.- \frac{R_{k-1}}{R_k}(\Delta R_k - \Delta R_{k-1})\right] \qquad (k = 2, \ldots, N-1)\end{aligned} \tag{17b}$$

$$\begin{aligned}p_N^0 &= P - \frac{R_{N-1}}{R_N}p_{(N-1)N}^0\\ &= P - c_N\frac{R_{N-1}}{R_N}(\Delta R_N - \Delta R_{N-1})\end{aligned} \tag{17c}$$

where $p^0_{i(i+1)}(i = 1, 2, \ldots, N-1)$ denotes the pressure on tube i due to tube $i+1$ prior to buckling, a uniform radial external pressure p on the multi-carbon nanotubes.

Combination of equations (15) and (17) gets

$$p_2^{0(N)} - p_2^{0(N-1)} -, \ldots, -p_2^{0(2)} - p_2^{0(1)} = pR_N. \tag{18}$$

All pressures p_l^0 and $p^0_{l(l+1)}$ can be determined from equations (16) and (17). Substitution of p_l^0 into equation (15) yields the relationships of $p_2^{0(l)}(l = 1, 2, \ldots, N)$, and then substitution of $p_2^{0(l)}$ into equation (18) yields the relationships of $p_2^{0(j)}$ and p.

Considering a simply supported multi-walled carbon nanotubes, its buckling mode is given by

$$u_3^{(l)} = A_l \sin \frac{m\pi x}{L} \cos n\theta \qquad (l = 1, 2, \ldots, N) \tag{19}$$

where A_l are real constants; L is the size of the double-walled carbon nanotube; and m and n, both positive integers, are the number of half-waves in the longitudinal direction and the circumferential wavenumber, respectively.

For the multi-walled carbon nanotubes, combination of equations (14) and (19) yields

$$\begin{aligned} &A_1\left[D(B_m^2+\eta_1^2)^4 + \frac{Eh}{R_1^2}B_m^4 - \frac{p_2^{0(1)}}{R_1}\eta_1^2(B_m^2+\eta_1^2)^2 \right.\\ &\quad\left. + c_1\eta_1^2(B_m^2+\eta_1^2)^2\right] - A_2c_1\eta_1^2(B_m^2+\eta_1^2)^2 \\ &\quad - 0.208DA_1a^2\varpi_1 = 0 \end{aligned} \tag{20a}$$

$$\begin{aligned} &A_j\left[D(B_m^2+\eta_j^2)^4 + \frac{Eh}{R_j^2}B_m^4 - \frac{P_2^{0(j)}}{R_j}\eta_j^2(B_m^2+\eta_j^2)^2 \right.\\ &\quad\left. + (c_j+c_{j-1})\eta_j^2(B_m^2+\eta_j^2)^2\right] - A_{j+1}c_j\eta_j^2(B_m^2+\eta_j^2)^2 \\ &\quad - A_{j-1}c_{j-1}\eta_j^2(B_m^2+\eta_j^2)^2 - 0.208DA_ja^2\varpi_j = 0 \end{aligned} \tag{20b}$$

$$\begin{aligned} &A_N\left[D(B_m^2+\eta_N^2)^4 + \frac{Eh}{R_N^2}B_m^4 - \frac{p_2^{0(N)}}{R_N}\eta_N^2(B_m^2+\eta_N^2)^2 \right.\\ &\quad\left. + c_{N-1}\eta_N^2(B_m^2+\eta_N^2)^2\right] - A_{N-1}c_{N-1}\eta_N^2(B_m^2+\eta_N^2)^2 \\ &\quad - A_N 0.208a^2D\varpi_N = 0 \end{aligned} \tag{20c}$$

where $B_m = \frac{m\pi}{L}$, $\eta_j = \frac{n}{R_j}(j = 1, 2, 3, \ldots, N)$, and the expressions of $\varpi_1, \varpi_j, \varpi_N$ are given as

$$\begin{aligned} \varpi_1 &= (B_m^2+\eta_1^2)\{[(B_m^2+\eta_1^2)(B_m^6+\eta_1^6)] + (2-\nu)B_m^2\eta_1^2\} \\ \varpi_j &= (B_m^2+\eta_j^2)\{[(B_m^2+\eta_j^2)(B_m^6+\eta_j^6)] + (2-\nu)B_m^2\eta_j^2\} \\ \varpi_N &= (B_m^2+\eta_N^2)\{[(B_m^2+\eta_N^2)(B_m^6+\eta_N^6)] \\ &\quad + (2-\nu)B_m^2\eta_N^2\}. \end{aligned}$$

Equations (20) can be written in matrix form:

$$(\mathbf{M}_1 + \mathbf{M}_0)\mathbf{A} = \mathbf{0} \tag{21}$$

where $\mathbf{M}_1$, $\mathbf{M}_0$ and A are given by

$$\begin{aligned} \mathbf{M}_1 &= \mathrm{diag}\left(D(B_m^2+\eta_l^2)^4 + \frac{Eh}{R_l^2}B_m^4 - \frac{P_2^{0(j)}}{R_l}\eta_l^2(B_m^2+\eta_l^2)^2 \right.\\ &\quad\left. - 0.208Da^2\varpi_l, l = 1, \ldots, N\right) \\ \mathbf{M}_0 &= \hbar_{l=1}^{N}(\mathbf{c}_l)\eta_l^2(B_m^2+\eta_l^2)^2 \\ \mathbf{A} &= (A_1, A_2, \ldots, A_N)^{\mathrm{T}} \end{aligned}$$

where $\hbar$ is an assembly operator and the matrix $\mathbf{c}_l$ is

$$\mathbf{c}_l = \begin{bmatrix} c_l & -c_l \\ -c_l & c_l \end{bmatrix}$$

and $\mathbf{A}$ is a nonzero vector. Let

$$\det(\mathbf{M}_1 + \mathbf{M}_0) = 0. \tag{22}$$

Equation (22) can be written as

$$\varphi(p) = \sum_{k=0}^{N} a_k p^k = 0. \tag{23}$$

The smallest real root of equation (23) is the critical buckling pressure for the multi-walled carbon nanotubes.

For $N = 2$, the critical axial buckling pressure can be obtained from equation (23), which gives

$$p = \frac{Y - \sqrt{Y^2 - 4XZ}}{2X} \tag{24}$$

where

$$\begin{aligned} X &= \eta_1^2\eta_2^2H_1H_2(B_m^2+\eta_1^2)^2(B_m^2+\eta_2^2)^2 \\ Y &= (s_2 - T_2)\eta_1^2H_1(B_m^2+\eta_1^2)^2 \\ &\quad + (s_1 - T_1)\eta_2^2H_2(B_m^2+\eta_2^2)^2 \\ Z &= (s_1 - T_1)(s_2 - T_2) - c^2\eta_1^2\eta_2^2(B_m^2+\eta_1^2)^2(B_m^2+\eta_2^2)^2. \end{aligned}$$

When the effect of small size-scale is neglected, equation (24) can be reduced to the classic (local) result:

$$\begin{aligned} &P_{\mathrm{cr}} \\ &= \frac{s_2\eta_1^2H_1(B_m^2+\eta_1^2)^2 + s_1\eta_2^2H_2(B_m^2+\eta_2^2)^2 - \sqrt{U^2+4V^2}}{2X} \end{aligned} \tag{25}$$

where

$$\begin{aligned} U &= s_2\eta_1^2H_1(B_m^2+\eta_1^2)^2 - s_1\eta_2^2H_2(B_m^2+\eta_2^2)^2 \\ V &= c\eta_1^2\eta_2^2\sqrt{H_1H_2}(B_m^2+\eta_1^2)^2(B_m^2+\eta_2^2)^2. \end{aligned}$$

The expressions of s_1, s_2, H_1, H_2 are given as

$$\begin{aligned} s_1 &= D(B_m^2+\eta_1^2)^4 + \frac{Eh}{R_1^2}B_m^4 + c\eta_1^2(B_m^2+\eta_1^2)^2 \\ T_1 &= 0.208a^2D(B_m^2+\eta_1^2)\{[(B_m^2+\eta_1^2)(B_m^6+\eta_1^6)] \\ &\quad + (2-\nu)B_m^2\eta_1^2\} \\ s_2 &= D(B_m^2+\eta_2^2)^4 + \frac{Eh}{R_2^2}B_m^4 + c\eta_2^2(B_m^2+\eta_2^2)^2 \\ T_2 &= 0.208a^2D(B_m^2+\eta_2^2)\{[(B_m^2+\eta_2^2)(B_m^6+\eta_2^6)] \\ &\quad + (2-\nu)B_m^2\eta_2^2\} \\ H_1 &= \frac{-cR_1R_2^2}{cR_1^2 + cR_1R_2 - Eh}, \\ H_2 &= \frac{(Eh - cR_1^2)R_2}{cR_1^2 + cR_1R_2 - Eh}. \end{aligned}$$

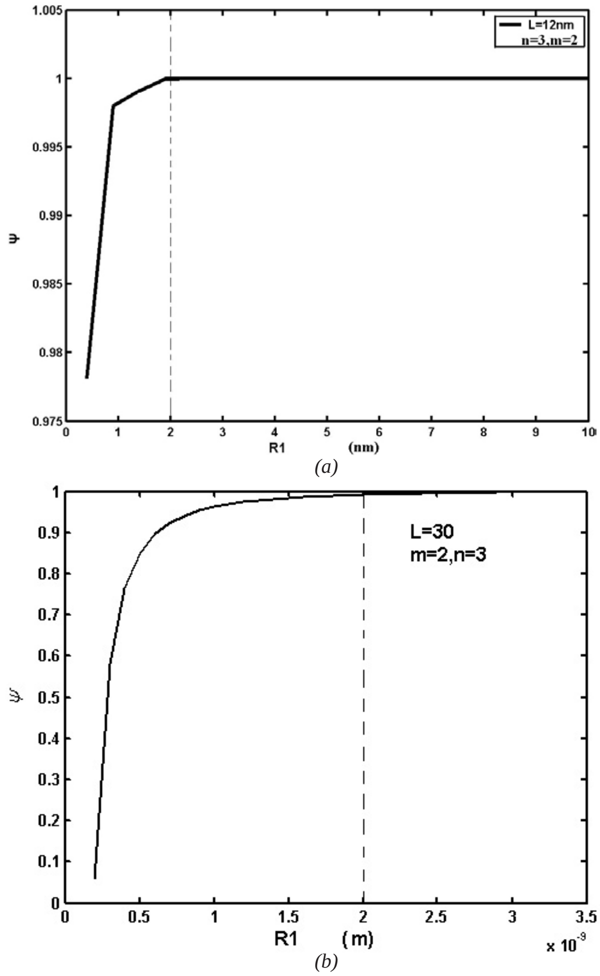

Figure 3. The ratio of ψ via the tube's inner radius R_1.

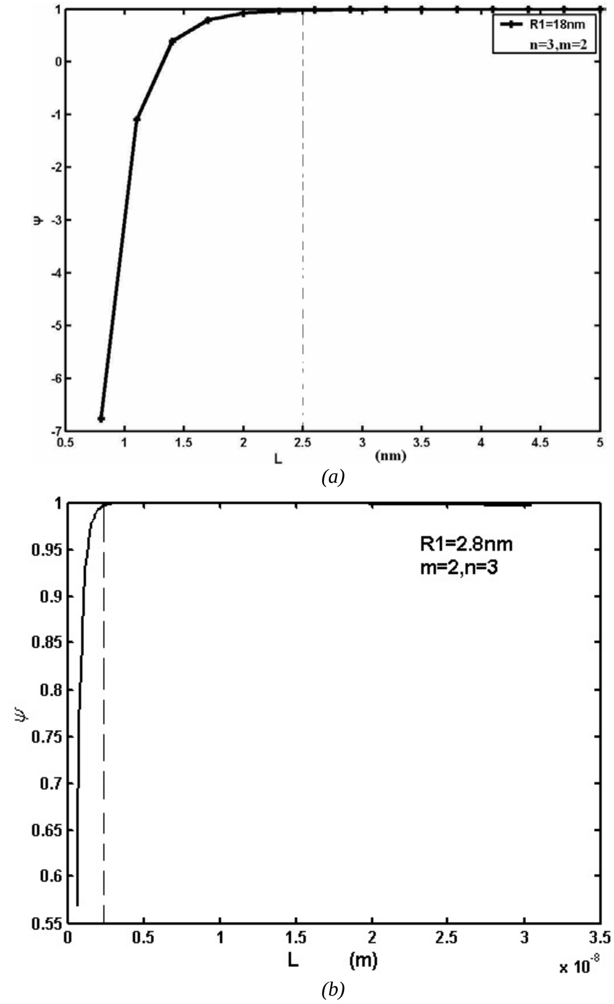

Figure 4. The ratio of ψ via the tube length L.

4. Numerical examples and discussions

In the numerical results, the effective bending stiffness is $D = 0.85$ eV, while the in-plane stiffness is $Eh = 360$ J m^{-2} (Yakobson *et al* 1996). In calculations, the size of a C–C bond is 0.142 nm, the Poisson's ratio of the material ν is 0.26, and the thickness of the carbon nanotube is $h = 0.34$ nm (Yoon *et al* 2003b).

To illustrate the influence of small size-scale on the critical radial buckling pressure of a double-walled carbon nanotube, the ratio ψ of the pressure predicted by equation (24) to that given by equation (25) is discussed:

$$\psi = \frac{p}{p_{\mathrm{cr}}} = \frac{Y - \sqrt{Y^2 - 4XZ}}{s_2\eta_1^2 H_1(B_m^2 + \eta_1^2)^2 + s_1\eta_2^2 H_2(B_m^2 + \eta_2^2)^2 - \sqrt{U^2 + 4V^2}}. \tag{26}$$

The closer the value of ψ is to 1, the smaller the effect of the small size-scale is; if ψ is equal to 1, the effect of the small size-scale will disappear.

Figures 3(*a*) and 3(*b*) show the relationship of the effect of the small size-scale on the radial buckling pressure of double-walled carbon nanotubes to its inner radius, R_1. It is observed from figure 3 that the effect of small size-scale on the radial buckling pressure decreases as the tube's inner radius R_1 increases, and the effect of the small size-scale will gradually disappear when the inner tube radius R_1 is beyond 2 nm.

Figures 4(*a*) and 4(*b*) imply the relationship between the ratio of ψ and the tube length L. It is obvious that the effect of small size-scale decreases as the tube length L increases. When the tube length reaches 2.5 nm, which is about 20 times of the inner feature length a, the effect of small size-scale will gradually disappear.

Figure 5 shows that the effects of small size-scale will increase with increases in buckling modes m and n if the effects of small size-scale exist in the radial and axial direction ($R_1 < 2$ nm, $L < 2.5$ nm). Figure 6 shows that the effects of small size-scale will increase with the increase in buckling mode m, and the effects of small size-scale will be independent of n if the effects of small size-scale disappear in the radial direction ($R_1 > 2$ nm). Figure 7 shows that, if the effects of small size-scale disappear in the axial direction ($L > 2.5$ nm), the effects of small size-scale will increase with an increase in buckling mode n, and the effects of small size-scale will remain invariable even if m varies. Figure 8 reveals that, when the effects of small size-scale disappear in the radial and the

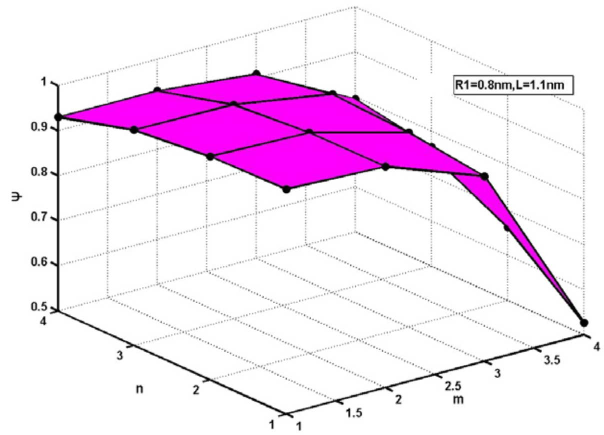

Figure 5. The effect of small size-scale via the tube modes m and n.

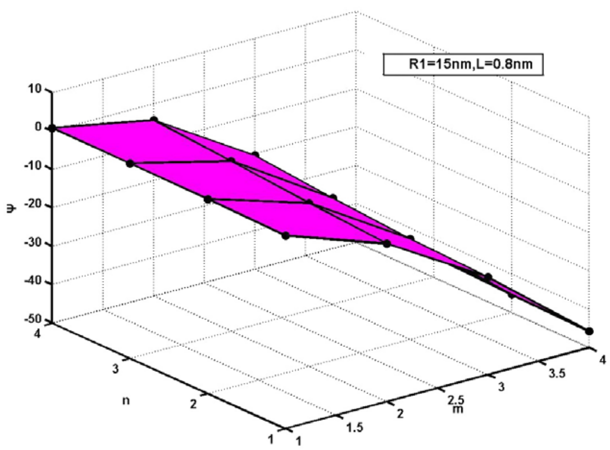

Figure 6. The effect of small size-scale via the tube modes m and n.

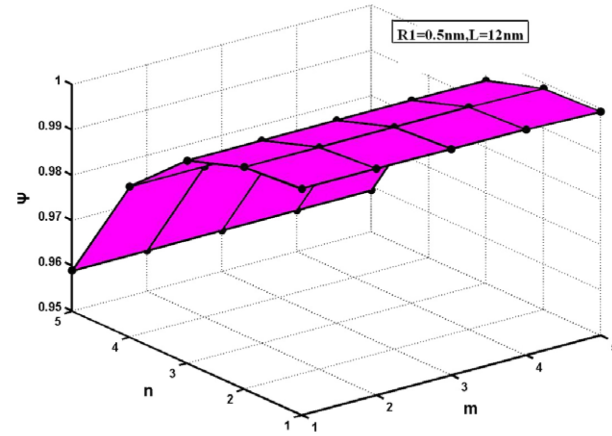

Figure 7. The effect of small size-scale via the tube modes m and n.

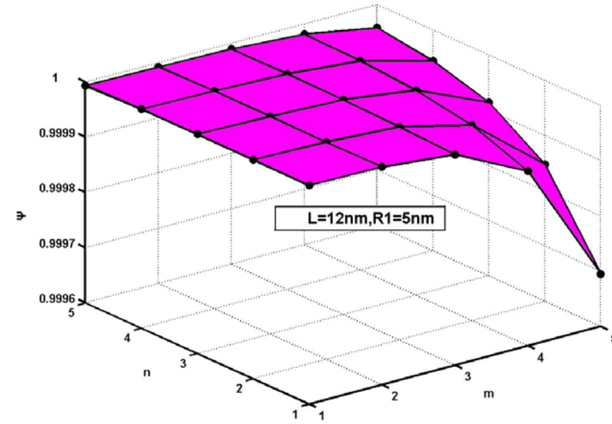

Figure 8. The effect of small size-scale via the tube modes m and n.

axial directions, the effects of small size-scale will disappear if the effects of small-size scale disappear in the radial and the axial directions. This can be interpreted as follows. The effects of small size-scale result from the long-range force. The long-range force exists only among these atoms whose distance is within a critical range. There is no force between two atoms when their distance exceeds the critical range. Therefore, there is a critical size of CNTs for which the effects of small size-scale disappears.

5. Conclusions

A nonlocal multi-walled shell model has been developed for the radial buckling of multi-walled carbon nanotubes under a uniform external radial pressure. Based on the theory of nonlocal elasticity, the average stresses of a representative element volume act as the nonlocal stress; the basic equations of a shallow shell are given.

The influence of small size-scale on the critical radial buckling pressure is discussed. It is revealed that the buckling pressure is influenced by the small size-scale. The effect of the small size-scale is dependent on the buckling mode, length and radius of the carbon nanotubes. The effects of small size-scale will disappear when the size of CNTs exceeds a critical size.

Acknowledgment

This work is supported by the National 973 number 2004 CB719402, NCET-04-0766, the National Science Foundation of China under grant number 10372031 and 10572048.

References

Cheng X-S 1989 *Application of Plate and Shell Theory* (Shan Dong Science and Technique) pp 534–7

Donnell L H 1933 Stability of thin walled tubes under torsion *NACA Report* No. 479

Eringen A C 1972 Linear theory of nonlocal elasticity and dispersion of plane waves *Int. J. Eng. Sci.* **10** 425–35

Eringen A C and Edelen D G B 1972 On nonlocal elasticity *Int. J. Eng. Sci.* **10** 233–8

Li C Y and Chou T-W 2003a A structural mechanics approach for the analysis of carbon nanotubes *Int. J. Solids Struct.* **40** 2487–99

Li C Y and Chou T W 2003b Multiscale modeling of carbon nanotube reinforced polymer composites *J. Nanosci. Nanotechnol.* **3** 423–30

Li C Y and Chou T-W 2004 Modeling of elastic buckling of carbon nanotubes by molecular structural mechanics approach *Mech. Mater.* **36** 1047–55

Lourie O, Cox P M and Wagner H D 1998 Buckling and collapse of embedded carbon nanotubes *Phys. Rev. Lett.* **81** 1638–41

Love A E H 1888 The small free vibrations and deformations of a thin elastic shell *Phil. Trans. R. Soc.* A 495–546

Maruyama B and Alam K 2002 Carbon nanotubes and nanofibers in composite materials *SAMPE J.* **38** 59–68

Peddieson J, Buchanan R and McNitt R P 2003 Application of nonlocal continuum models to nanotechnology *Int. J. Eng. Sci.* **41** 305–12

Peigney A, Laurent Ch, Flahaut E and Rousset A 2000 Carbon nanotubes in novel ceramic matrix nanocomposites *Ceram. Int.* **26** 667–83

Price N M, Liu M and Eatock Taylor R 1998 Vibrations of cylindrical pipes and open shells *J. Sound Vib.* **218** 361–87

Ru C Q 2000 Column buckling of multiwalled carbon nanotubes with interlayer radial displacements *Phys. Rev.* B **62** 16962–7

Ru C Q 2001 Radially compressed buckling of a doublewalled carbon nanotube embedded in an elastic medium *J. Mech. Phys. Solids* **49** 1265–79

Schadler L S, Giannaris S C and Ajayan P M 1998 Load transfer in carbon nanotube epoxy composites *Appl. Phys. Lett.* **73** 3842–4

Wang Q and Varadan V K 2005 Stability analysis of carbon nanotubes via continuum models *Smart Mater. Struct.* **14** 281–6

Wong E W, Sheehan P E and Lieber C M 1997 Nanobeam mechanics: elasticity, strength, and toughness of nanorods and nanotubes *Science* **277** 1971–5

Yakobson B I, Brabec C J and Bernholc J 1996 Nanomechanics of carbon tubes instabilities beyond linear range *Phys. Rev. Lett.* **76** 2511–4

Yoon J, Ru C and Mioduchowski A 2003a Sound wave propagation in multiwall carbon nanotubes *J. Appl. Phys.* **93** 4801–6

Yoon J, Ru C Q and Mioduchowski A 2003b Vibration of an embedded multi-wall carbon nanotubes *Compos. Sci. Technol.* **63** 1533–42